Reference : Soil Dynamics(Shamsher Prakash, Professor of Civil Engineering University of Missouri-Rolla, McGraw-Hill Book Company, 1981)

CHAPTER
FOUR

DYNAMIC STRESS DEFORMATION AND STRENGTH CHARACTERISTICS OF SOILS

4.1 INTRODUCTION

Several problems in engineering practice require knowledge of the dynamic soil properties. Generally, dynamic foundation problems are divided into either small strain amplitude or large strain amplitude response. For example, foundations for a radar tracking station can tolerate only very small levels of strain while structures in earthquake or blast damage areas must be able to tolerate large strain levels.

A variety of field and laboratory methods have been developed for evaluating dynamic soil properties. The major soil properties that need to be ascertained in soil dynamics and geotechnical earthquake engineering are:

1. Shear strength evaluated in terms of strain rates and stress-strain characteristics
2. Dynamic moduli, Young's modulus, shear modulus, bulk modulus, and constrained modulus
3. Poisson's ratio
4. Damping
5. Liquefaction parameters: cyclic shearing stress ratio, cyclic deformation, and pore-pressure response

In this chapter, conventional static soil tests are summarized first, followed by a detailed discussion of laboratory and field methods used for determining

the relevant dynamic soil properties. Values of the dynamic soil moduli for typical soils are presented also.

Liquefaction and parameters associated with liquefaction are discussed in Chap. 8.

4.2 CONVENTIONAL SOIL TESTS UNDER STATIC LOADS

Because diverse rock-weathering processes cause soils to be formed in nature, no human agency has control over the properties of soils. This is the main difference between soils and conventional building materials, such as steel and concrete, whose properties are almost tailor-made.

In addition, soils at any given site are not homogeneous, either areally or with regard to depth. It is therefore absolutely essential that soil tests be performed at all construction sites to evaluate the strength and other pertinent properties of the soils.

In all laboratory strength tests, it is of paramount importance that field loading conditions be reproduced as accurately as possible. This requires that field anisotropy, strain rate, and drainage condition be modeled. Testing problems are more difficult as rates of strain increase as in dynamic problems.

Equipment for testing soils under static loading conditions has been somewhat standardized for a long time. It is desirable to describe briefly the conventional equipment and the types of tests that can be performed.

Although a number of methods are available for shear-testing of soils, the most commonly used are the direct shear test and the triaxial compression test.

Before describing the actual tests and their interpretations, it is necessary to discuss drainage conditions, which have a very important bearing on the shear strength of soils.

4.3 DRAINAGE DURING SHEAR TESTS

Most soil deposits whose shear strengths are to be determined will be saturated at some time during the design life of the structure. Drainage conditions before and during shear influence the shear strength of saturated soils. In shear tests, soils are first subjected to normal or confining stress, which is usually maintained constant. An increasing shear stress is then applied until failure occurs. Shear tests have been devised to measure the shear strength of soils under three different limiting drainage conditions, as discussed below:

1. *Unconsolidated-undrained test or "quick test"*: In these tests, no drainage is permitted under applied normal or confining load, or during shear. Thus, the normal load is not transferred to the soil grains as intergranular pressure but exists as a hydrostatic excess pore pressure. It cannot, therefore, mobilize any frictional resistance. Preventing drainage during shear prevents volume changes that might otherwise take place.

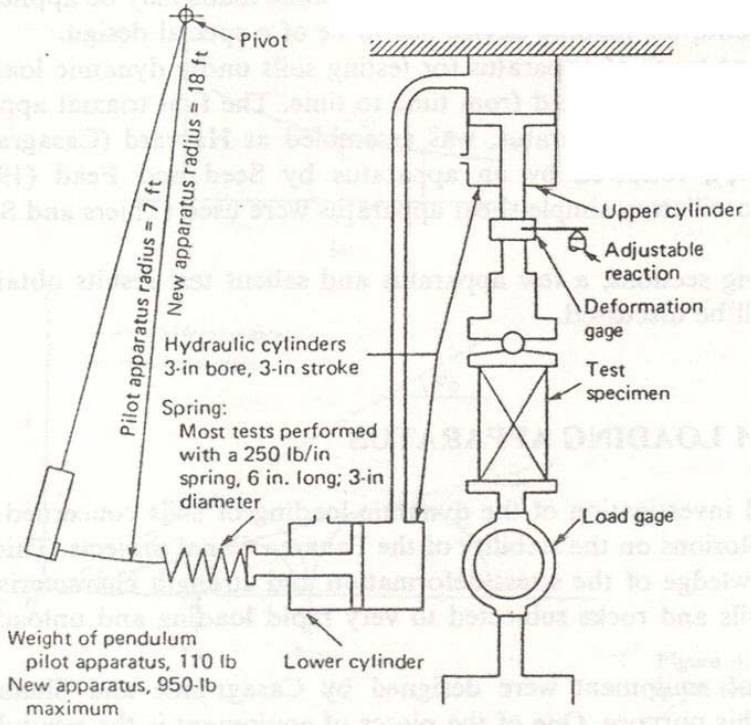

Figure 4.6 Pendulum loading apparatus. *(After Casagrande and Shannon, 1948b.)*

static loads and can be used in a dynamic test. Similarly, a deformation gauge was constructed on a cantilever metal strip with electric-resistance strain gauges mounted on one end while the other end rested on an unmoveable support. The strain introduced in the cantilever was a measure of the deformation of the soil sample.

Two typical soils tested, Cambridge clay and Manchester sand, have the

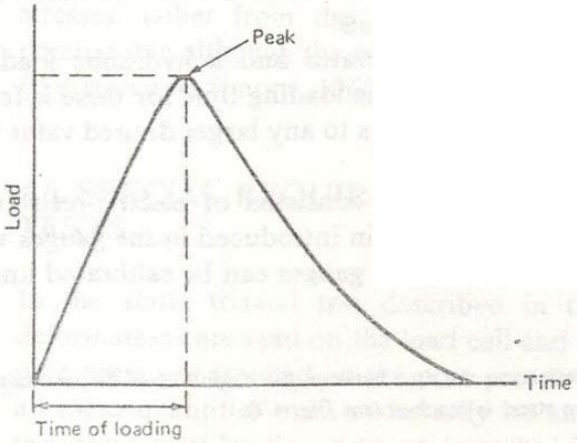

Figure 4.7 Time of loading in transient tests.

following properties:

Cambridge clay

natural moisture content	30 – 50%
liquid limit	37 – 59%
plastic limit	20 – 27%

The tests were performed both in the unconfined and confined state.

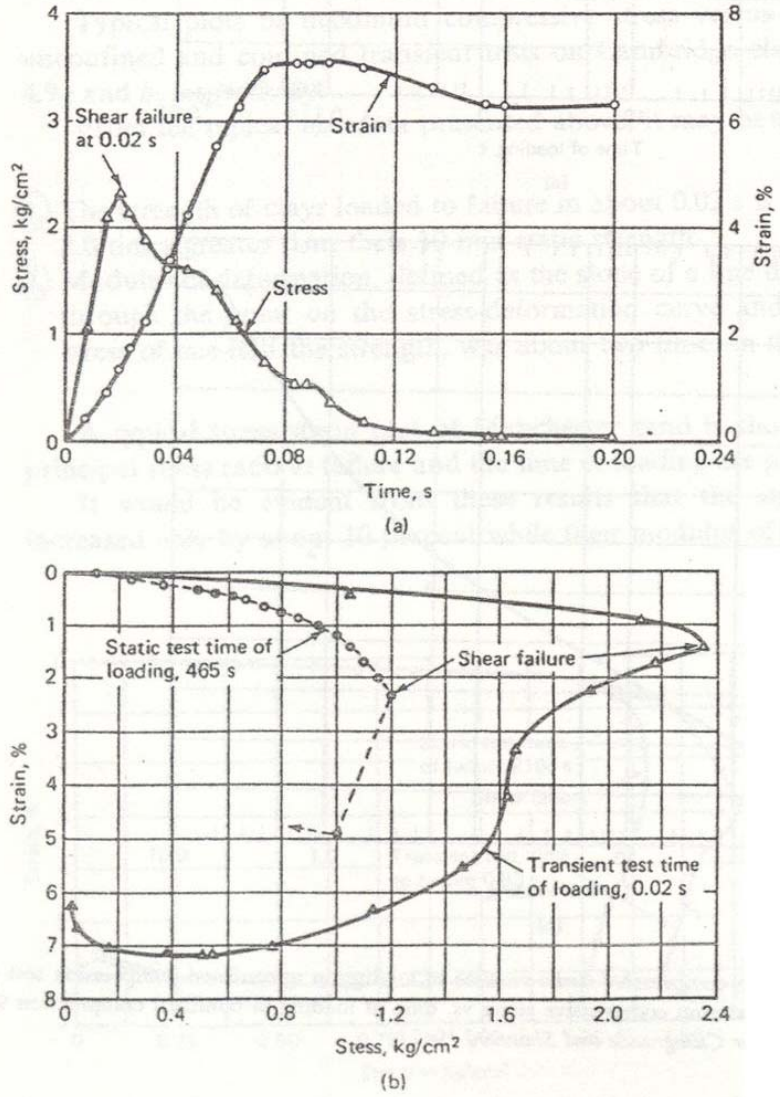

Figure 4.8 (*a*) Time vs. stress and strain in an unconfined transient test on Cambridge clay. (*b*) Stress vs. strain in transient test with time of loading of 0.02 s and a static test on Cambridge clay. *(After Casagrande and Shannon, 1949.)*

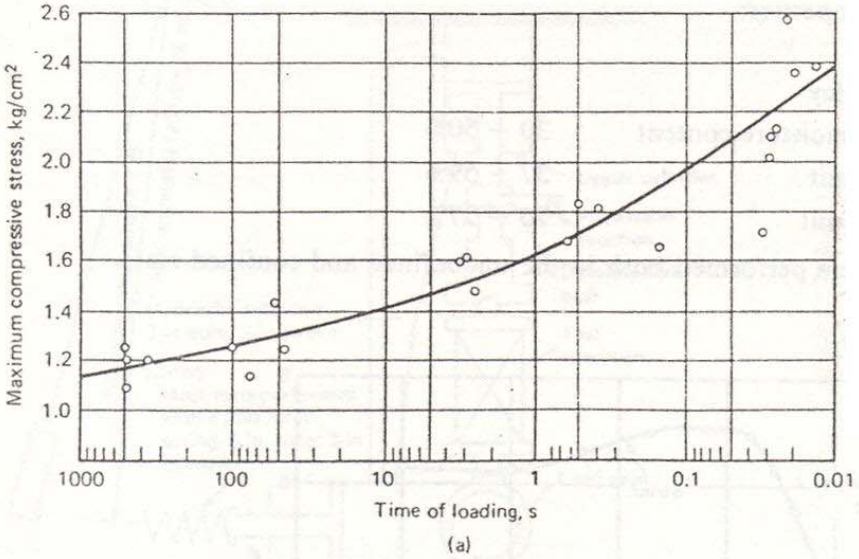

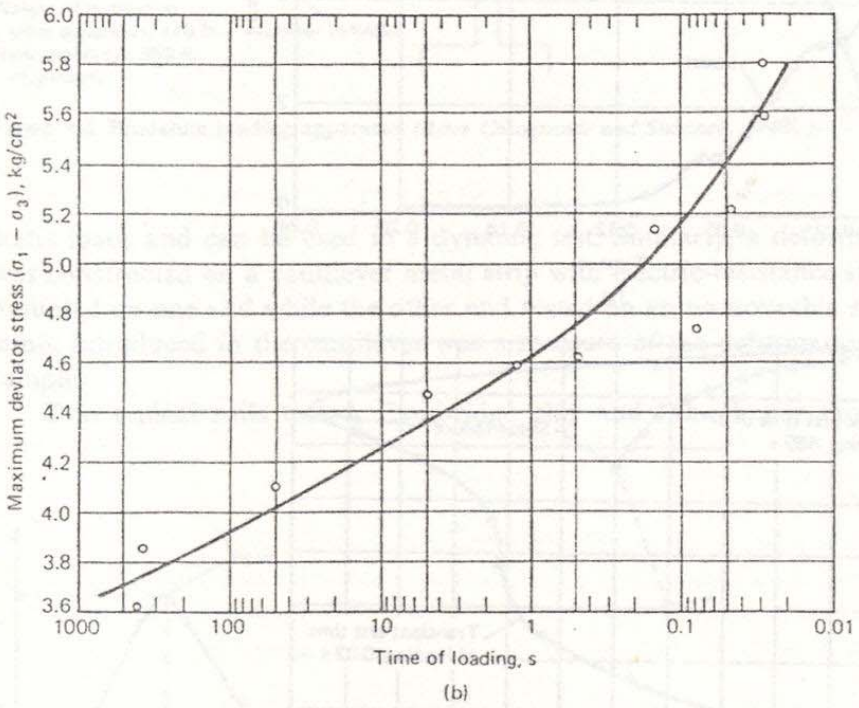

Figure 4.9 (*a*) Maximum compressive stress vs. time of loading in unconfined compression test on Cambridge clay. (*b*) Maximum compressive stress vs. time of loading in confined compression test on Cambridge clay. *(After Casagrande and Shannon, 1949.)*

Manchester sand

grain size	between 0.42 and 0.21 mm
maximum void ratio	$e_{max} = 0.88$
minimum void ratio	$e_{min} = 0.61$

Figure 4.8*a* shows a simultaneous plot of stress and strain versus time in a test with a time of loading of 0.02 s obtained from an unconfined transient compression test on Cambridge clay. The stress-strain relationship is plotted in Fig. 4.8*b* along with a stress-strain plot for a static test in which time of loading was 465 s.

Typical plots of maximum compressive stress versus time of loading for unconfined and confined transient tests on Cambridge clay are shown in Fig. 4.9*a* and *b*, respectively.

From the typical test data presented above, it may be concluded that:

1. The strength of clays loaded to failure in about 0.02 s is approximately 1.5 to 2.0 times greater than their 10-min static strength.
2. Modulus of deformation, defined as the slope of a line drawn from the origin through the point on the stress-deformation curve and corresponding to a stress of one-half the strength, was about two times in the transient tests.

A typical stress-strain plot of Manchester sand is shown in Fig. 4.10. The principal stress ratio at failure and the time of loading are plotted in Fig. 4.11.

It would be evident from these results that the strength of the sands increased only by about 10 percent while their modulus of deformation was not

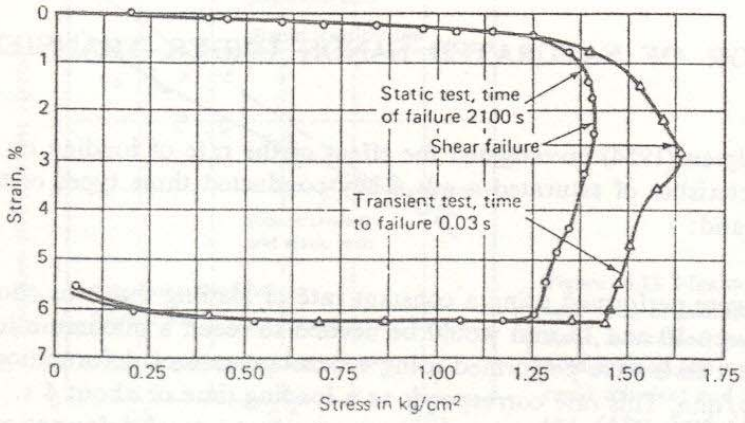

Figure 4.10 Stress vs. strain of Manchester sand in a transient test and static test. *(After Casagrande and Shannon, 1949.)*

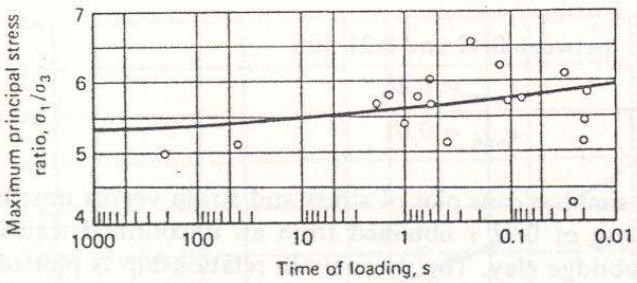

Figure 4.11 Maximum principal stress ratio vs. time of loading of Manchester sand in transient tests. *(After Casagrande and Shannon, 1949.)*

time-dependent. These investigations suffer from the following shortcomings:

1. The dynamic load was not superimposed on a static load (Tschebotarioff, 1949). Certain static shearing stresses are always present in an embankment.
2. At best, the transient loading adopted in these investigations represents only one cycle of earthquake loading. Sometimes there may be as many as 100 peaks in an actual earthquake.
3. Finally, the sands were tested while dry and dense. The effect of dynamic loading on saturated loose sands may induce large pore pressures resulting in loss of strength and consequent partial or complete liquefaction of sands. This aspect of the problem is of great practical importance.

Saturated sands were studied by Seed and Lundgren (1954) under transient loads. Salient results of their investigation shall now be presented.

4.8 BEHAVIOR OF SATURATED SANDS UNDER TRANSIENT LOADING

Seed and Lundgren (1954) investigated the effect of the rate of loading on the strength characteristics of saturated sands. They conducted three types of tests on a uniform sand:

1. Static tests were performed using a constant rate of loading that was chosen so that between 10 and 15 min would be needed to reach a maximum load.
2. Slow transient tests were performed using a constant rate of deformation of 15 cm (6 in)/min. This rate corresponds to a loading time of about 4 s.
3. Rapid transient tests were performed using a constant rate of deformation of about 100 cm (40 in)/s. This rate corresponds to a loading time of about 0.02 s.

In slow transient tests, a testing machine with a platform of a travel rate of up to 15 cm/min was used. An impact testing machine was used to apply loads in rapid transient tests. This impact machine consists of a 22.7-kg (50-lb) weight that is allowed to fall in guides from any desired height onto the test specimen. In these tests, the weight was allowed to fall from a height of 10 cm (4 in) before striking a spring on top of the loading piston. The weight then traveled 2.5 cm (1 in) before its movement was arrested by wooden stops. At the time the weight struck the spring at the piston, it was traveling at a rate of about 300 cm/s (120 in/s). The change in velocity of the weight after striking the loading piston was negligible, and test data indicate that this impact test produced a very nearly constant rate of deformation.

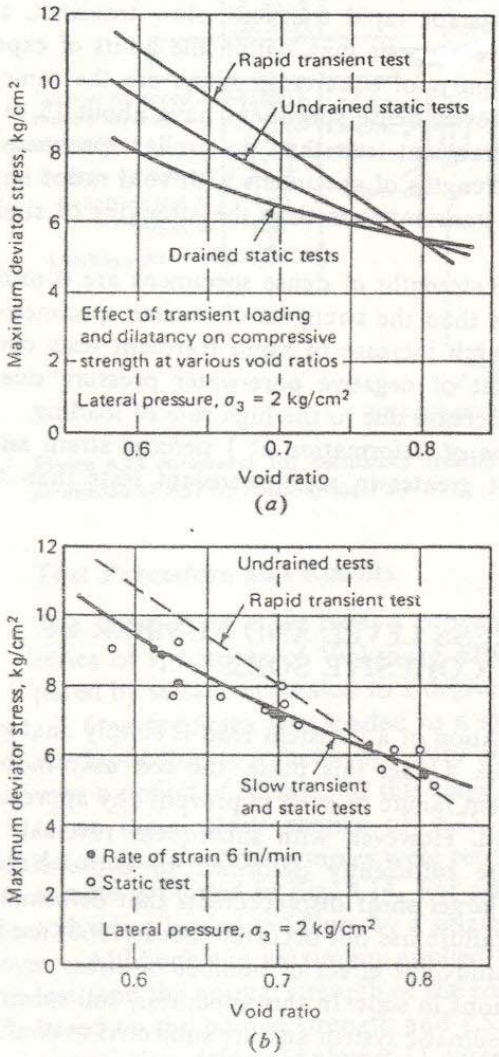

Figure 4.12 Maximum deviator stress vs. void ratio of Sacramento sand. (*a*) Drained static, undrained static, and rapid transient, both drained and undrained. (*b*) Undrained rapid transient and slow transient and static test. *(After Seed and Lundgren, 1954. Reprinted with permission of ASTM, Philadelphia, Pa.)*

Test Results

Figure 4.12*a* shows a plot of maximum deviator stress versus void ratios for drained static, undrained static, and rapid transient tests in both drained and undrained conditions.

This figure suggests that undrained static strength is greater than drained static strength, since negative pore-water pressures develop in dense sand. As the void ratio increases, the difference in the two strengths reduces, and at $e \approx 0.8$, the two strengths are equal. This value corresponds to the critical void ratio (Casagrande, 1936). Also, it was found that strengths were not materially different in rapid undrained and drained tests. This would seem to indicate that, although provisions were made for drainage to take place in the drained tests, the rate of loading was so fast that there was no time for drainage to occur.

Figure 4.12*b* shows similar plots for rapid transient, slow transient, and static tests, all undrained. This figure suggests that, within the limits of experimental error, the strengths of specimens of equal void ratios are the same in static and slow transient tests. However, dense specimens have about 15 to 20 percent greater strengths in rapid transient tests than do similar specimens in static or slow transient tests. The strengths of specimens with void ratios larger than about 0.8 are lower in rapid transient tests than the strengths of similar specimens in static tests.

Figure 4.12 also shows that the strengths of dense specimens are considerably greater in rapid transient tests than the strengths of similar specimens in static drained tests. Thus, the strength increase in rapid transient tests comes from two sources: the development of negative pore-water pressure due to dilatancy effects and the strength increase due to the high rate of loading.

It was also found that modulus of deformation at 1 percent strain and 2 percent strain is about 30 percent greater in rapid transient tests than that determined in static tests.

4.9 EFFECT OF STATIC STRESS LEVEL AND NUMBER OF PULSES ON STRENGTH OF COHESIVE SOILS

As discussed previously, the application of a transient load is simply analogous to the first pulse of an earthquake. Under this pulse, the soil may mobilize enough additional strength to prevent failure or even to prevent any appreciable permanent deformation of the soil. However, with subsequent reversals and continued stress, the soil may be sufficiently deformed to cause either a reduction in soil strength or such larger shear displacements that deformations are readily apparent even though failure has not occurred. Seed (1960) used the apparatus shown in Fig. 4.13 to study the effect of number of stress reversals and other factors on the deformations in soils. In this apparatus, soil specimens are dynamically loaded using a pneumatic system and are subjected to confining pressure in a triaxial cell (Seed and Fead, 1959).

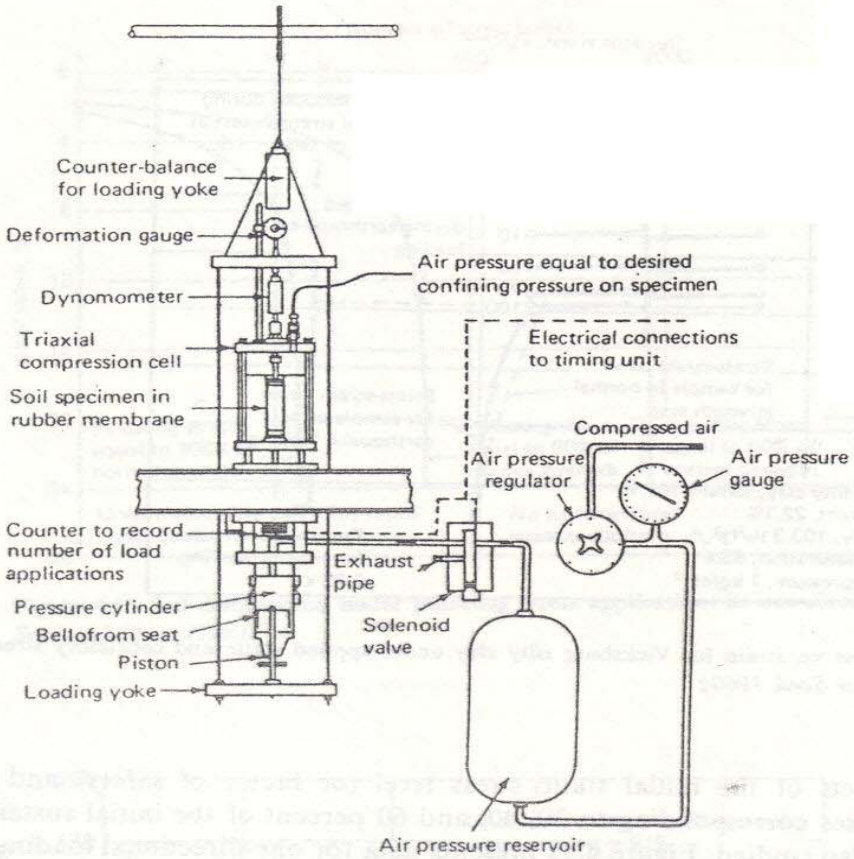

Figure 4.13 Apparatus for oscillatory triaxial test. *(After Seed and Fead, 1959. Reprinted with permission of ASTM, Philadelphia, Pa.)*

Test Procedure and Results

The stress-strain curve from a conventional static test is shown in Fig. 4.14. A series of specimens of Vicksburg silty clay of identical composition were prepared by static compaction to a degree of saturation of about 95 percent.

One specimen was loaded to a stress equal to 66 percent of this strength, corresponding to a factor of safety of 1.5, and allowed to come to equilibrium over a period of 30 min. At this stage, 100 transient stress pulses, corresponding to an initial stress change of ±35 percent, were applied, and the resulting deformations of the samples were recorded. The stress-strain relationship for the sample is plotted in Fig. 4.14. For purposes of comparison, the strength of the soil, when loaded to failure by a single transient stress application, is also shown.

Although the maximum applied stress, including the earthquake stress, is less than the normal strength of the soil (in fact, the lowest safety factor was 1.12 based on the normal strength and 1.52 based on the transient strength), the soil nevertheless deformed almost 11 percent during the transient stress applications.

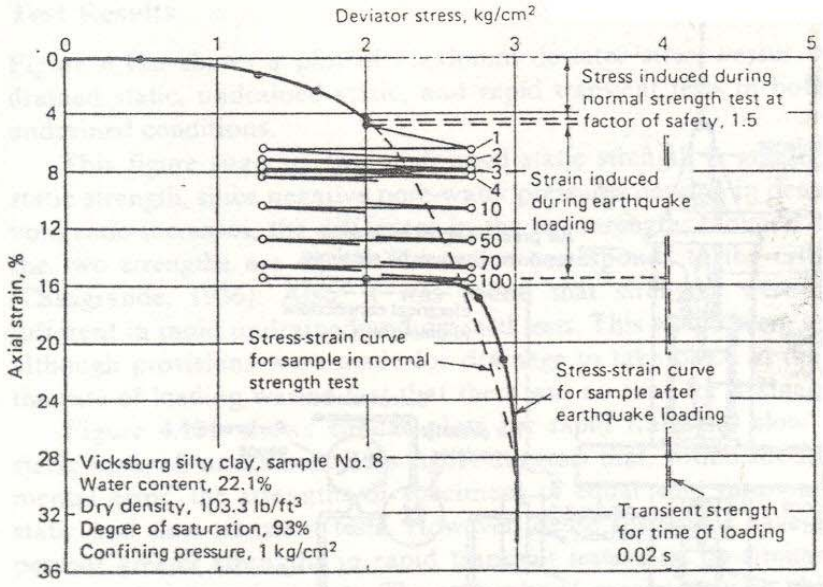

Figure 4.14 Stress vs. strain for Vicksburg silty clay under applied static and oscillatory stress in triaxial test. *(After Seed, 1960.)*

The effects of the initial static stress level (or factor of safety) and the transient pulses corresponding to 20, 40, and 60 percent of the initial sustained stress were also studied. Figure 4.15 presents data for one-directional loading on three samples of an undisturbed saturated silty clay of medium sensitivity [San Francisco Bay mud, liquid limit (LL) = 88, plastic limit (PL) = 43]. Stress levels equal to 100, 80, and 60 percent of the normal strength of the clay (that is, the strength determined in a conventional undrained test) were applied to the three samples. The samples were able to support these stresses for different numbers of stress reversals, but ultimately each sample failed completely. The number of pulses causing failure can readily be determined from Fig. 4.15. It is interesting to note that, even for a stress level of as low as 60 percent of the normal strength of the soil, 900 transient applications induced failure of this material.

From the data presented in Fig. 4.15, a determination was made of the relationship between the magnitude of the pulsating stress and the number of stress pulses required to cause failure for the special case of no sustained stress (Seed and Chan, 1966). This relationship is shown by the upper curve in Fig. 4.16. Failure was induced by any desired number of pulses by using different stress levels to complete the full range of this relationship.

Three samples were also subjected to a sustained stress equal to 47 percent of their normal strengths, and, when creep movement had essentially stopped, different levels of pulsating stresses were superimposed. In this case, the pulsating stress levels used were 115, 60, and 40 percent of the normal strength; they induced failure after 1, 9, and 88 stress applications, respectively. Plotting this data leads to a second curve in Fig. 4.16.

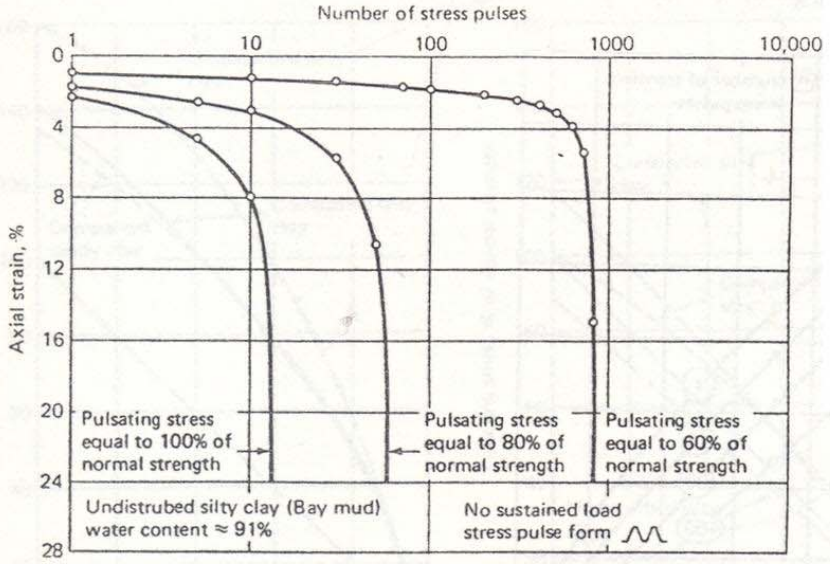

Figure 4.15 Soil deformation under pulsating stress applications in one-directional loading. *(After Seed and Chan, 1966.)*

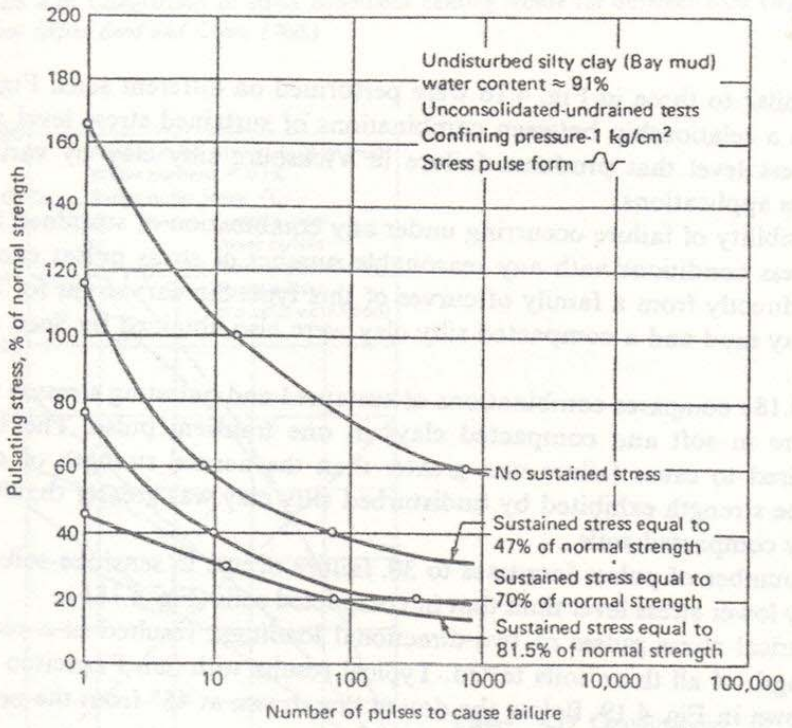

Figure 4.16 Relationship between stress level and number of pulses causing failure in one-directional loading. *(After Seed and Chan, 1966.)*

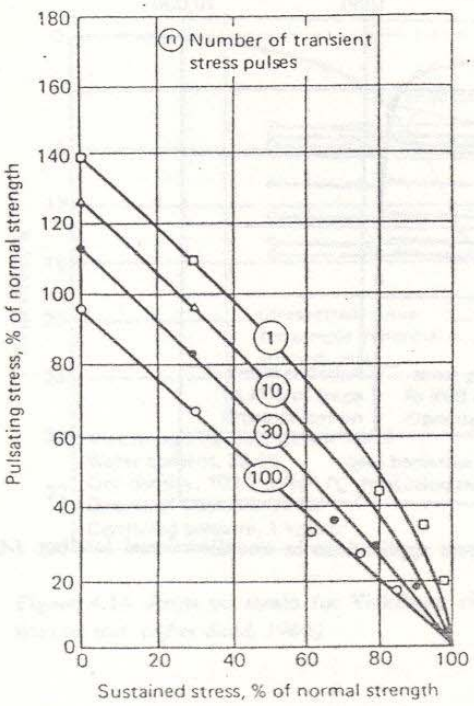

Figure 4.17 Combination of sustained and pulsating stress intensities causing failure in Vicksburg silty clay. *(After Seed and Chan, 1966.)*

Tests similar to those in Fig. 4.16 were performed on different soils. Figure 4.17 presents a relationship between combinations of sustained stress level and pulsating stress level that produces failure in Vicksburg silty clay by various selected stress applications.

The possibility of failure occurring under any combination of sustained and pulsating stress conditions with any reasonable number of stress pulses can be determined directly from a family of curves of this type. Similar curves for San Francisco Bay mud and a compacted silty clay were also obtained by Seed and Chan (1966).

Figure 4.18*a* compares combinations of sustained and pulsating stresses that induce failure in soft and compacted clays in one transient pulse. The total stress† required to cause failure was greater than the normal strength of each soil. Also, the strength exhibited by undisturbed silty clay was greater than that displayed by compacted soils.

As the number of pulses increases to 30, failure occurs in sensitive soil at a considerably lower stress level than that in compacted soils (Fig. 4.18*b*).

Symmetrical stress pulses of two-directional loadings‡ resulted in a reduction in strength of all three soils tested. Typical results with San Francisco Bay mud are shown in Fig. 4.19. Below the dotted line drawn at 45° from the origin,

† Defined as sustained stress + pulsating stress.
‡ See Sec. 1.3.

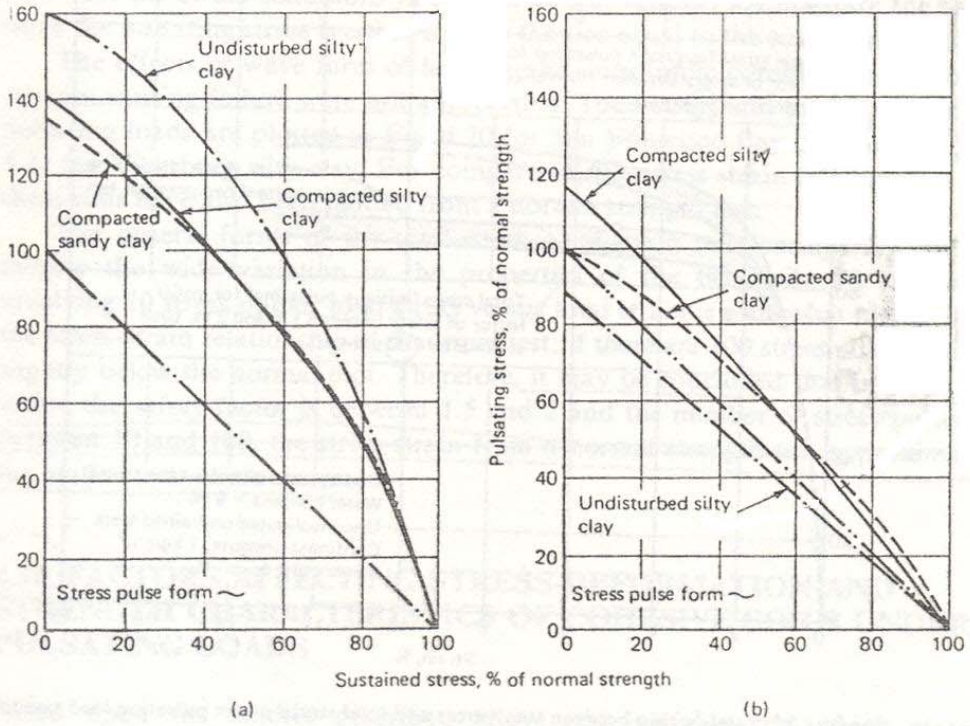

igure 4.18 Comparison of stress conditions causing failure for different soils. (*a*) 1 pulse. (*b*) 30 ılses. *(After Seed and Chan, 1966.)*

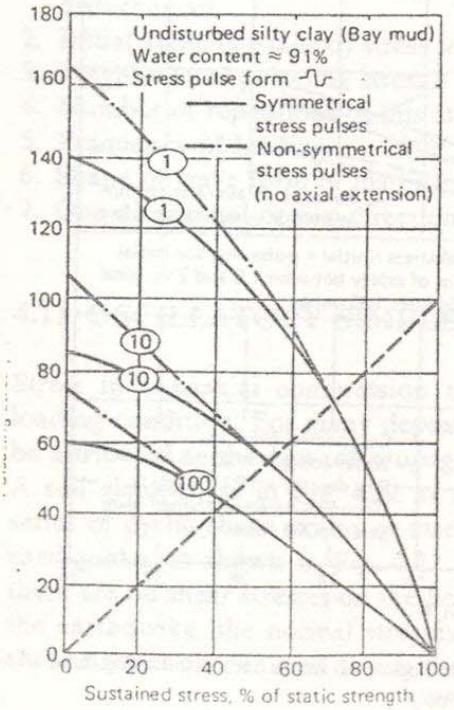

Figure 4.19 Combinations of sustained and pulsating stresses causing failure—one- and two-directional loading in San Francisco Bay mud. *(After Seed and Chan, 1966.)*

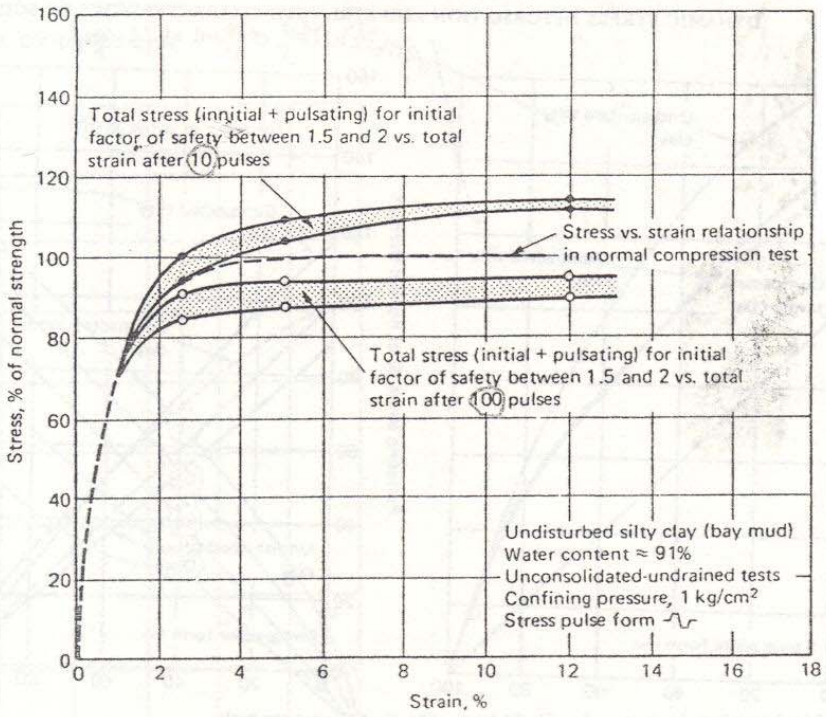

Figure 4.20 Relationship between total stress and total strain under pulsating load conditions in San Francisco Bay mud. *(After Seed and Chan, 1966.)*

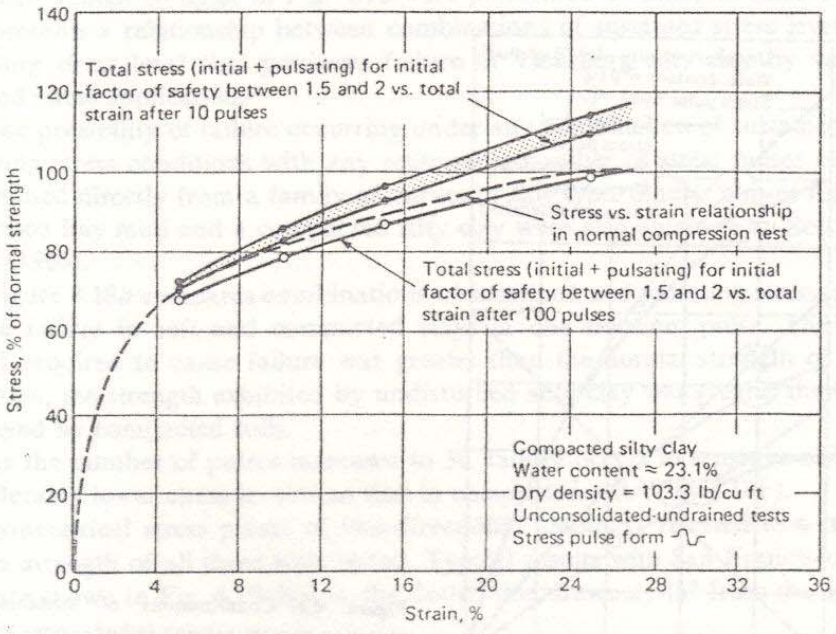

Figure 4.21 Relationship between total stress and total strain under pulsating load conditions in Vicksburg silty clay. *(After Seed and Chan, 1966.)*

ıote that the stress conditions in one- or two-directional loadings are the same ;ince the pulsating stress is either smaller than or equal to the sustained stress.

The effects of wave form of loading and anisotropic consolidation on total ;tresses causing failure were not appreciable. Total stress and total strain under ɔulsating loads are plotted in Fig. 4.20 for San Francisco Bay mud and in Fig. 4.21 for Vicksburg silty clay. For comparison, the stress-strain relationships for these soils have also been plotted from a normal strength test.

The general forms of the total-stress–total-strain relationships are similar despite the wide variation in the properties of the two soils. In situations involving 10 stress pulses, total stress versus total strain is somewhat higher than the stress-strain relationship of a normal test; if there are 100 stress pulses, this is slightly below the normal plot. Therefore, it may be concluded that in all cases, where the safety factor is between 1.5 and 2 and the number of stress pulses is between 10 and 100, the stress-strain from a normal strength test approximates the static stress-strain curve.

4.10 FACTORS AFFECTING STRESS-DEFORMATION AND STRENGTH CHARACTERISTICS OF COHESIVE SOILS UNDER PULSATING LOADS

Based upon the studies described above, the variables on which stress-deformation and strength characteristics of the cohesive soils depend are summarized below:

1. Type of soil and its properties (for example, water content, γ_d, and state of disturbance)
2. Initial static (sustained) stress level
3. Magnitude of pulsating stress
4. Number of repetitions of this stress
5. Frequency of loading
6. Shape of wave form of loading
7. One-directional or two-directional loading

4.11 OSCILLATORY SIMPLE SHEAR TEST

Stress in a triaxial compression test does not adequately simulate the field loading condition. For many deposits, a major part of the soil deformation may be attributed to the upward propagation of shear waves from underlying layers. A soil element, as in Fig. 4.22 at *xx*, may be considered to be subjected to a series of cyclic shear strains or stresses that may reverse many times during an earthquake, as shown in Fig. 4.23. In the case of a horizontal ground surface, there are no shear stresses on the horizontal plane before the earthquake. During the earthquake, the normal stresses on this plane remain constant while cyclic shear stresses are induced during the period of shaking.

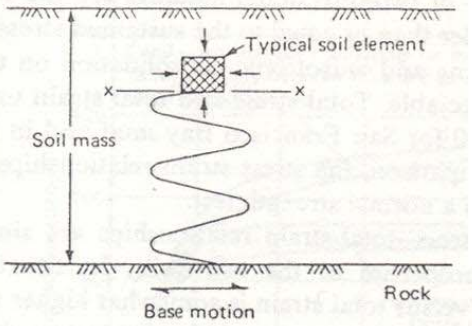

Figure 4.22 Transmission of shear waves from rock base into the overlying soil.

Other field conditions that differ from those developed in triaxial compression tests are as follows (Peacock and Seed, 1968):

1. In the field, there is a cyclic reorientation of the principal stress directions. The major principal stress is initially vertical and rotates through some angle θ, to the right and left of its initial position. In a triaxial compression test, the major principal stress can act only in either the vertical or horizontal direction.
2. In the field, the soil element is initially consolidated to k_0 condition.
3. In the field, deformations are presumed to occur under plane-strain conditions, while in a triaxial compression test, the intermediate principal stress is either equal to minor principal stress during axial compression or equal to major principal stress during lateral compression.

The simple shear device consists essentially of a simple box, an arrangement for applying a cyclic load to the soil, and an electronic recording system. The box of Roscoe (1953), which contains a square sample with a side length of 6 cm and a thickness of about 2 cm, is provided with two fixed side walls and two hinged end walls so that the sample may be subjected to deformations of the type shown in Fig. 4.23. A schematic diagram in Fig. 4.24 illustrates how the end walls rotate simultaneously at the ends of the shearing chamber to deform the soil uniformly (Peacock and Seed, 1968). Kjellman (1951), Hvorslev and Kaufman (1952), Bjerrum and Landra (1966), and Prakash, Nandkumaran, and Joshi (1973) have described the apparatus fabricated respectively at their centers.

Test data from simple shear tests have been analyzed to determine shear parameters, soil moduli, and damping, as well as the liquefaction potential of loose sands (Chap. 8). Prakash, Nandkumaran, and Bansal (1974) reported test

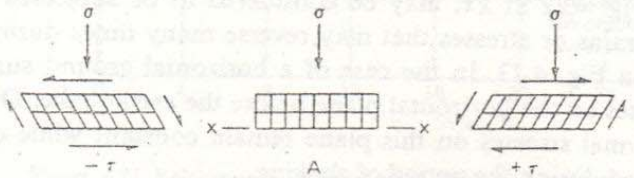

Figure 4.23 Idealized stress condition for element of soil below ground surface during an earthquake.

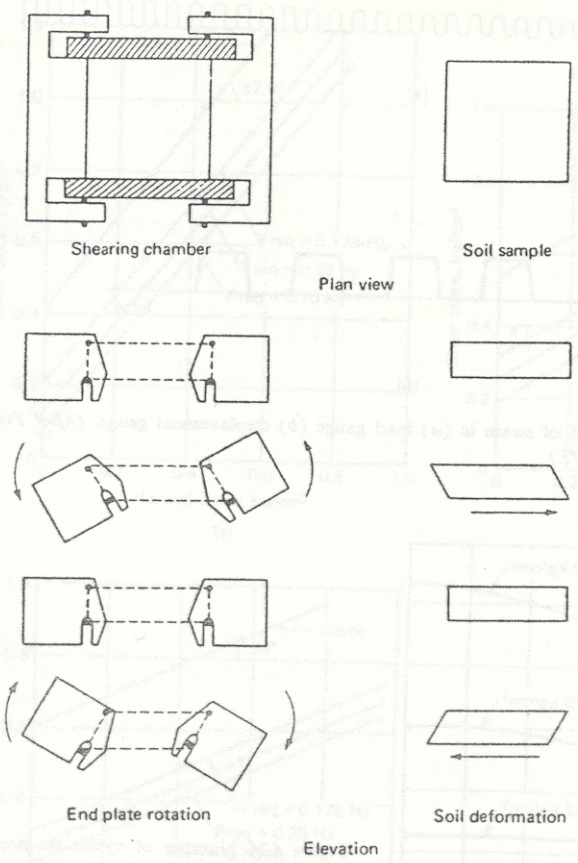

Figure 4.24 Schematic diagram illustrating rotation of hinged end plates and soil deformation in oscillatory simple shear. *(After Peacock and Seed, 1968.)*

data on three *artificial* soils (a mixture of sand and bentonite) compacted at their optimum moisture content in quick tests. Figure 4.25 shows time-dependent records of strains respectively in displacement gauge and the load gauge.

Figure 4.26 is a plot of the number of cycles versus horizontal deformation for sample 1. Plots are made for dynamic shear stress intensities of 0.182, 0.375, and 0.542 kg/cm^2. For all tests, the normal stress was 0.292 kg/cm^2 and the dynamic shear stress frequency was 0.175 Hz.

Figure 4.27 plots dynamic shear stress and horizontal displacement on sample 1 after 30 cycles of oscillatory stress under various normal stresses. Similar data were obtained for other samples and at frequencies of 0.35 Hz and 0.70 Hz.

Assuming that failure corresponds to 12-mm displacement, as for a direct shear test under static loads, Mohr strength envelopes for all three soils are

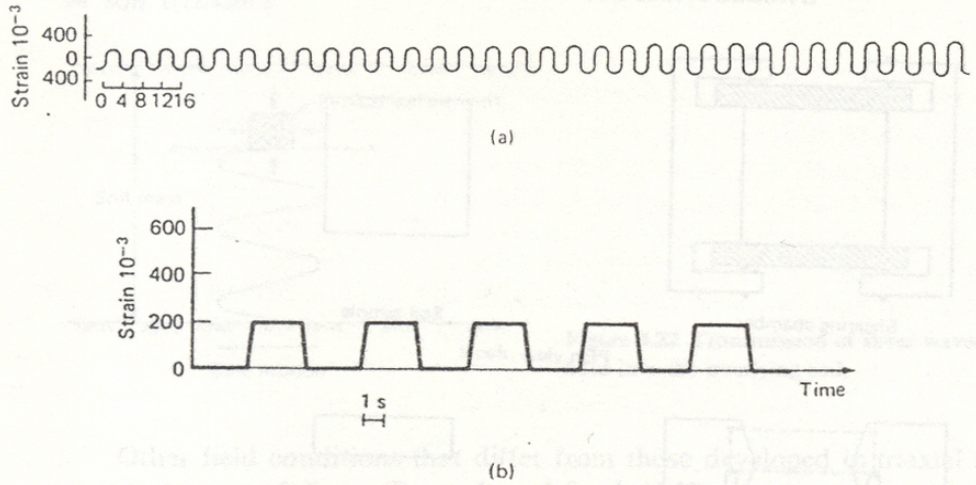

Figure 4.25 Timewise record of strain in (*a*) load gauge (*b*) displacement gauge. *(After Prakash, Nandkumaran, and Joshi, 1973.)*

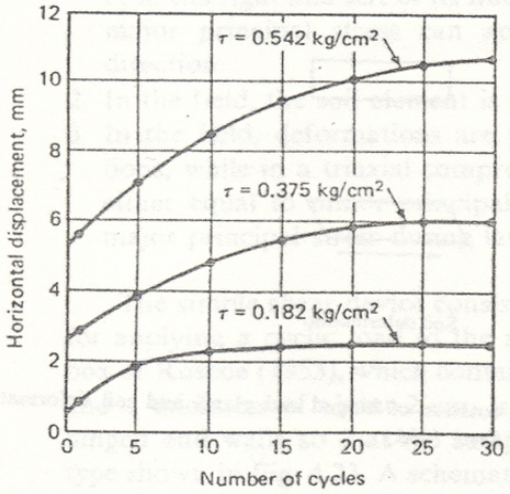

Figure 4.26 Number of cycles vs. horizontal displacement in oscillatory simple shear in sample no. 1 (σ_n = 0.292 kg/cm², f = 0.175 Hz). *(After Prakash, Nandkumaran, and Bansal, 1974.)*

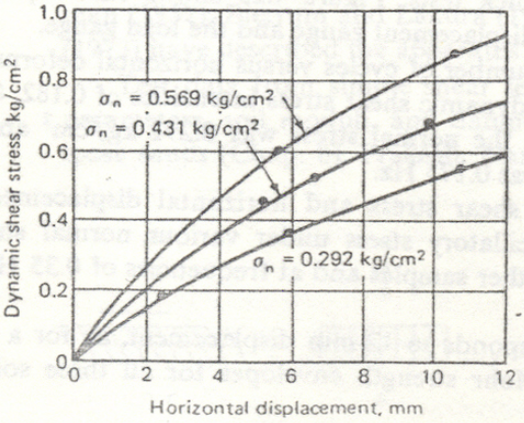

Figure 4.27 Dynamic shear stress vs. horizontal displacement in 30 cycles in sample no. 1. *(After Prakash, Nandkumaran, and Bansal, 1974.)*

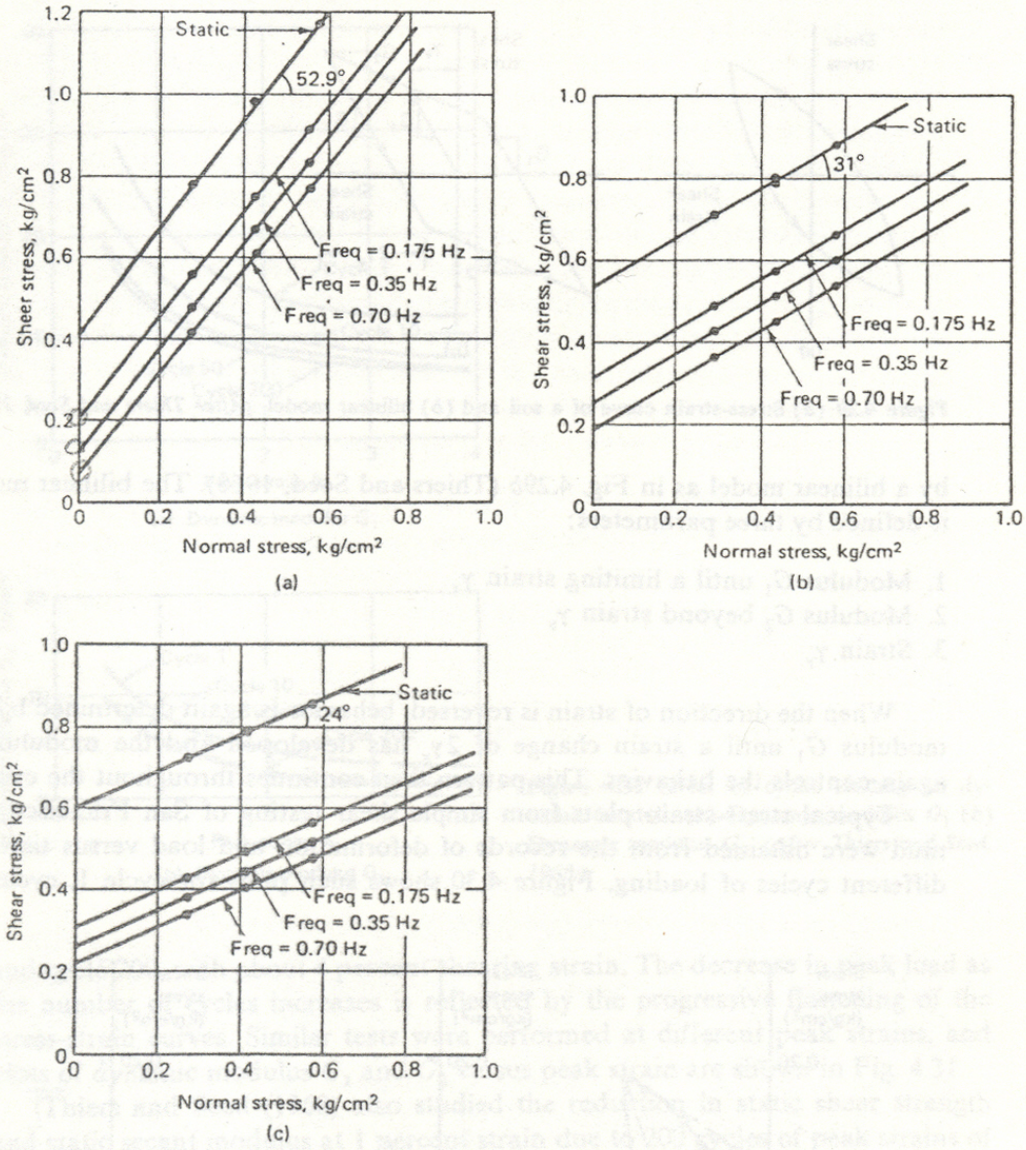

Figure 4.28 Mohr envelopes for static and dynamic stresses. (*a*) SM (*b*) CL (*c*) CH *(After Prakash, Nandkumaran, and Bansal, 1974.)*

plotted in Fig. 4.28. It can be seen from this figure that the strength parameter c is reduced under oscillatory tests while the angle of internal friction remains almost constant. The cohesion intercept decreases with increasing frequency. Also, the more compressible a soil, the larger the reduction in the cohesion parameter.

The shear-stress–shear-strain relationship may be as shown in Fig. 4.29*a*. The soils exhibit nonlinear stress-strain characteristics from the very beginning of the loading cycle. For purposes of analysis, this behavior may be represented

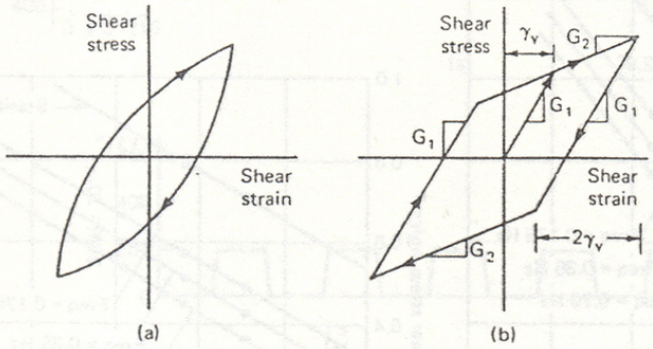

Figure 4.29 (*a*) Stress-strain curve of a soil and (*b*) bilinear model. *(After Thiers and Seed, 1968.)*

by a bilinear model as in Fig. 4.29*b* (Thiers and Seed, 1968). The bilinear model is defined by three parameters:

1. Modulus G_1 until a limiting strain γ_Y
2. Modulus G_2 beyond strain γ_Y
3. Strain γ_Y

When the direction of strain is reversed, behavior is again determined by the modulus G_1 until a strain change of $2\gamma_Y$ has developed and the modulus G_2 again controls the behavior. This pattern then continues throughout the cycle.

Typical stress-strain plots from simple shear testing of San Francisco Bay mud were obtained from the records of deformation and load versus time for different cycles of loading. Figure 4.30 shows such plots for cycle 1, cycle 50,

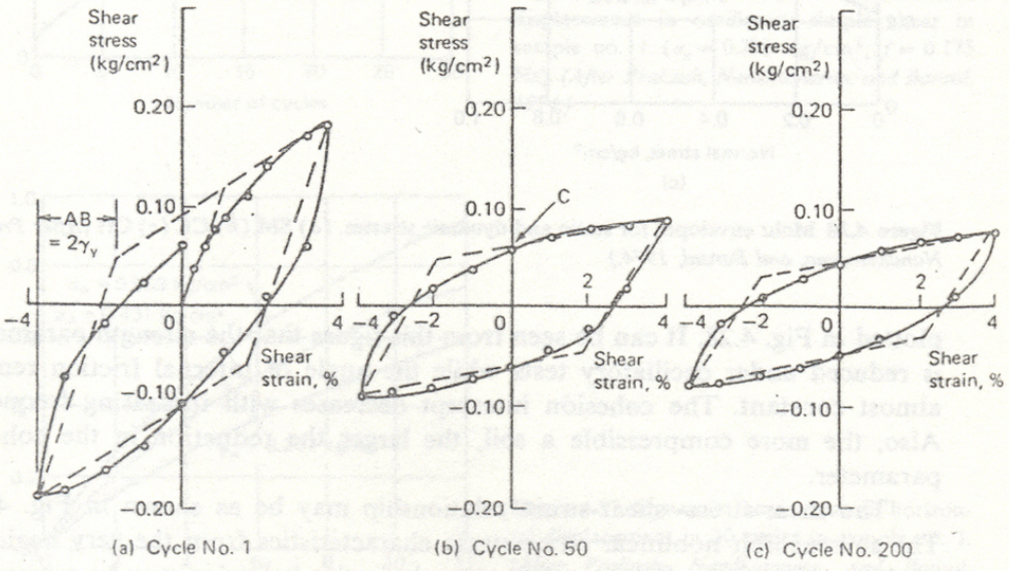

Figure 4.30 Stress-strain curves and bilinear models in San Francisco Bay mud. (*a*) Cycle no. 1. (*b*) Cycle no. 50. (*c*) Cycle no. 200. *(After Thiers and Seed, 1968.)*

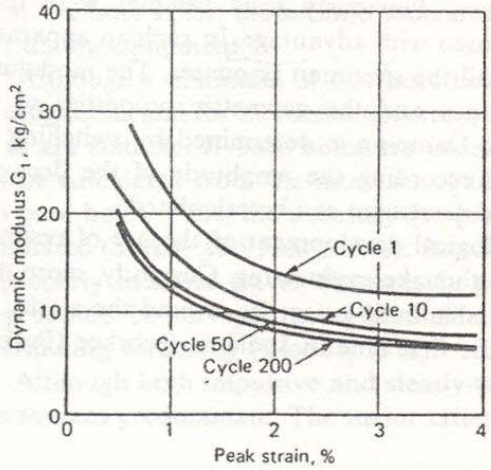

(a) Dynamic modulus G_1

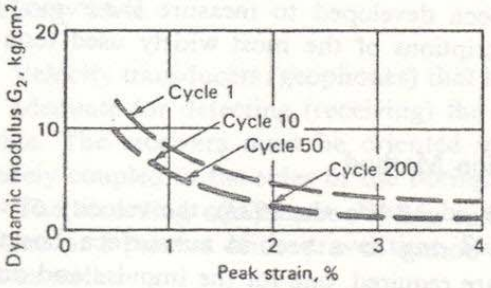

(b) Dynamic modulus G_2

Figure 4.31 Effect of cyclic loading on dynamic moduli. (*a*) Dynamic modulus G_1 (*b*) Dynamic modulus G_2. *(After Thiers and Seed, 1968.)*

and cycle 200, with about 4 percent shearing strain. The decrease in peak load as the number of cycles increases is reflected by the progressive flattening of the stress-strain curves. Similar tests were performed at different peak strains, and plots of dynamic modulus G_1 and G_2 versus peak strain are shown in Fig. 4.31.

Thiers and Seed (1968) also studied the reduction in static shear strength and static secant modulus at 1 percent strain due to 200 cycles of peak strains of different magnitude up to 4 percent and found that while strength reduction was only about 20 percent at 4 percent peak cyclic strain, the static modulus after cyclic loading decreased to about 50 percent of its initial value.

4.12 RESONANT COLUMN APPARATUS

The resonant column test for determining modulus and damping characteristics of soils is based on the theory of wave propagation in prismatic rods† (Richart, Hall, and Woods, 1970). Either compression waves or shear waves can be

† See Chap. 3.

Table 4.3 Values of k

PI	k
0	0
20	0.18
40	0.30
60	0.41
80	0.48
> 100	0.50

Equation (4.17) can be expressed in a more convenient form as follows:

$$G_{max} = \frac{A\,OCR^k}{F(e)}(p_a)^{1-n}(\bar{\sigma}_0)^n \tag{4.18}$$

By introducing p_a,† the parameter A is dimensionless, whereas $\bar{\sigma}_0$ and G_{max} in Eq. (4.17) are in lb/in^2 and the constant 1230 has the dimensions (lb/in^2)$^{0.5}$. It is also desirable to change the form of the void ratio function in Eq. (4.17) by letting

$$F(e) = 0.3 + 0.7e^2 \tag{4.19}$$

in Eq. (4.18). The function $F(e)$ is less complicated than the void ratio function in Eq. (4.17), but gives about the same effect as e in the range $0.4 < e < 1.2$. For very large values of e, Eqs. (4.18) and (4.19) give monotonically decreasing values of G_{max} while Eq. (4.17) gives $G_{max} = 0$ for $e = 2.973$, with G_{max} increasing for $e > 2.973$. Equations (4.18) and (4.19) will approximate Eq. (4.17) for $0.4 < e < 1.2$ by taking $n = 0.5$ and $A = 625$. Figure 4.40‡ shows a plot of $[G_{max}/(OCR)^k(p_a\bar{\sigma})^{0.5}]$ versus the void ratio from laboratory and field measurements (Hardin, 1978).

The elastic parameters required for computation of soil constant are k, n, and ν. For most purposes, it will suffice to use $\nu = 0.12$, $n = 0.5$, and values of k in Table 4.3. For preliminary analysis, Fig. 4.40 can be used as a guide (Hardin, 1978).

For clean sands, it was found that G is dependent on $\bar{\sigma}_0$ and e (Richart, 1977). Analytical expressions were presented for the shear modulus of clean sands as

$$G_{max} = 700\,\frac{(2.17 - e)^2}{1 + e}(\bar{\sigma}_0)^{0.5} \tag{4.20}$$

for round-grained sands ($e < 0.80$) and

$$G_{max} = 326\,\frac{(2.97 - e)^2}{1 - e}(\bar{\sigma}_0)^{0.5} \tag{4.21}$$

† p_a stands for atmospheric pressure.

‡ In this figure, s is a dimensionless elastic stiffness parameter in Hardin's (1978) proposed stress-strain relation for inherent isotropy. For clean sands, s varies from 1200 to 1500 and for silts and clays, s varies from 700 to 2000.

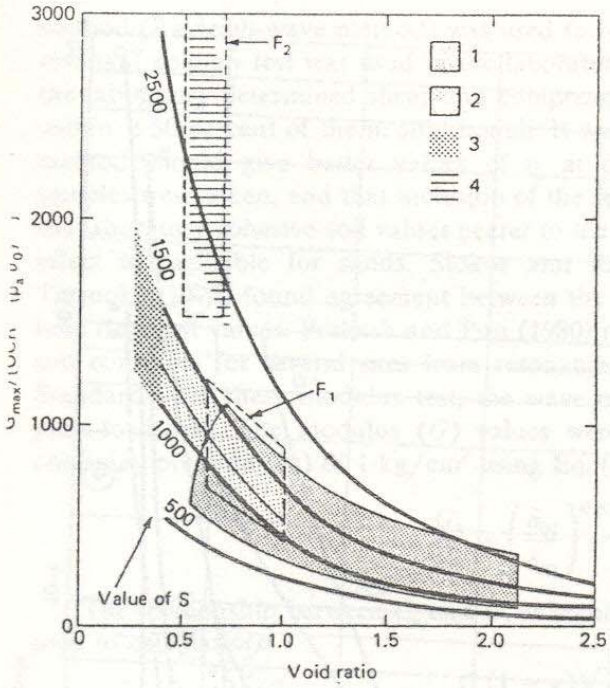

Figure 4.40 Elastic stiffness from laboratory and field measurements: 1—lab, silty sands, silts, and clays; 2—lab, clean sands; 3—lab, dense, well-graded gravel-sand with some fines; 4—lab, relatively uniform clean gravels; F_1—field, silty sands, silts, and clays at Ferndale, Cholame, and El Centro sites by SW-AA (1971); F_2—field, sands, silts, and clays at Anderson et al. (1978) sites A, B, and C. *(After Hardin, 1978.)*

for angular-grained sands. In Eqs. (4.20) and (4.21), G and $\bar{\sigma}_0$ have units of kilograms per square centimeter. Both equations were originally established to correspond to shearing strains of 10^{-4} or less. Equation (4.20) gave values slightly lower than those obtained by pulse tests (Whitman and Lawrence, 1963). Iwasaki and Tatsuoka (1977) recently determined experimentally that

$$G_{max} = 900 \frac{(2.17 - e)^2}{1 + e} (\bar{\sigma}_0)^{0.38} \tag{4.22}$$

from tests on clean sands ($0.61 < e < 0.86$ and $0.2 < \sigma_0 < 5$ kg/cm^2) at shearing strain amplitudes of 10^{-6}. For shearing strains for 10^{-4}, their results agreed with Eq. (4.20).

Comparison of G from Different Tests

Several comparisons have been made among G_{max} values obtained by different tests in the field and in the laboratory.

Cunny and Fry (1973) reported on laboratory and field evaluations of G_{max} at 14 sites which contained a variety of soils. The steady-state surface vibration

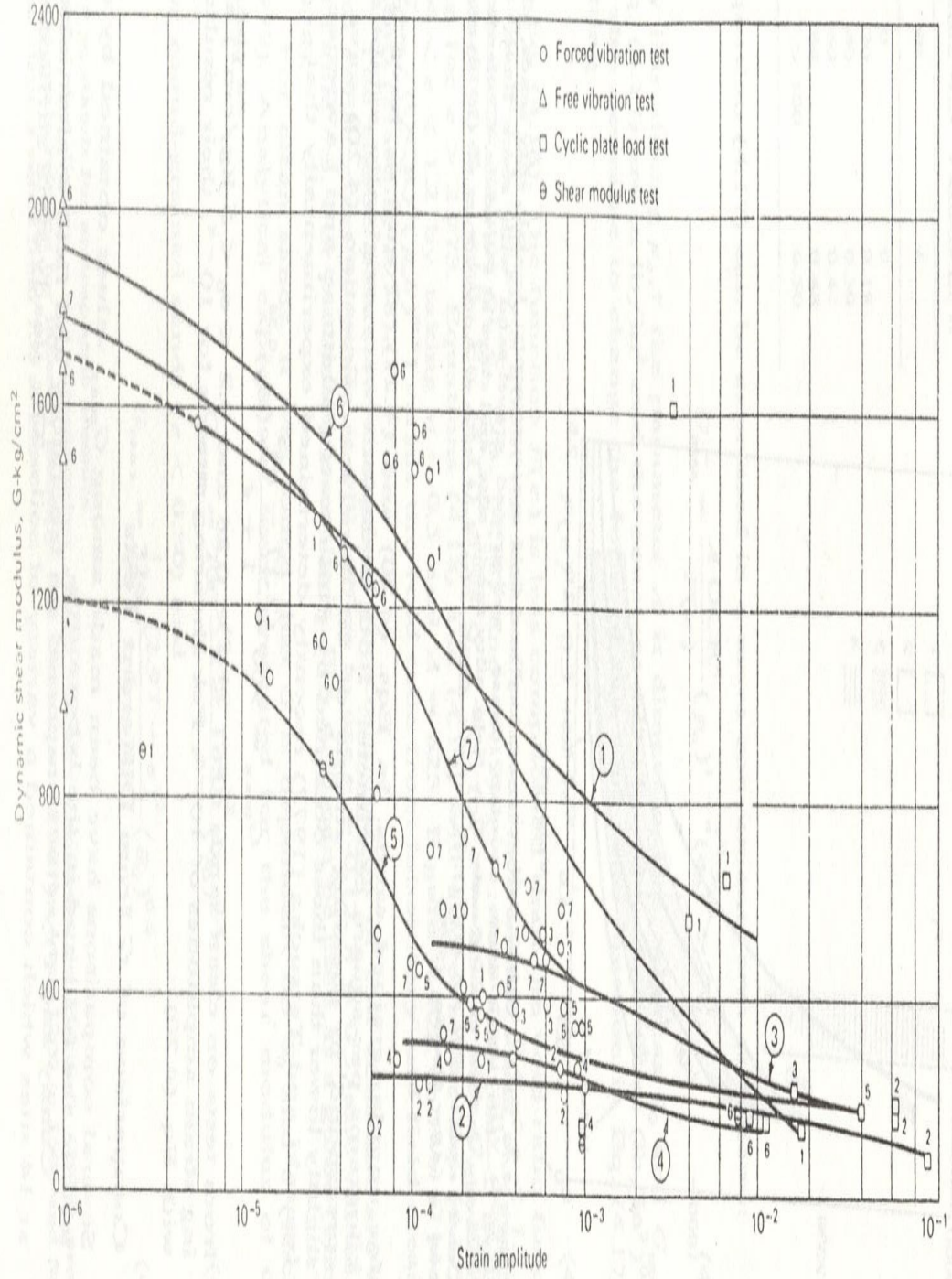

Figure 4.41 Dynamic shear modulus vs. strain. *(After Prakash and Puri, 1980.)*

method (Rayleigh-wave method) was used for evaluating G_{max} in the field. The resonant column test was used in the laboratory. From evaluation of test data, the laboratory-determined shear and compression moduli were found to range within ±50 percent of the in situ moduli. It was pointed out that the cross-hole method should give better values of v_s at depths from which undisturbed samples were taken, and that inclusion of the secondary time effect would bring the laboratory cohesive-soil values nearer to the field values. The secondary time effect is negligible for sands. Stokoe and Richart (1973) and Iwasaki and Tatsuoka (1977) found agreement between the resonant column and the cross-hole field test values. Prakash and Puri (1980) reported in situ data on dynamic soil constants for several sites from resonance tests on blocks, as per Indian Standards, the shear modulus test, the wave propagation test, and the cyclic-plate-load test. The modulus (G) values were reduced to a mean effective confining pressure ($\bar{\sigma}_0$) of 1 kg/cm^2 using Eq. (4.23):

$$\frac{G_1}{G_2} = \left(\frac{\bar{\sigma}_{01}}{\bar{\sigma}_{02}}\right)^{0.5} \tag{4.23}$$

The relationship between C_u and G, as recommended by Barkan (1962), was used to calculate G:

$$G = \frac{C_u(1-\nu)\sqrt{A}}{2.26} \tag{4.24}$$

in which A = area of contact and ν = Poisson's ratio.

The detailed values of shear moduli for the seven sites are shown in Table 4.4. A plot of G versus strain is shown in Fig. 4.41. A plot of normalized

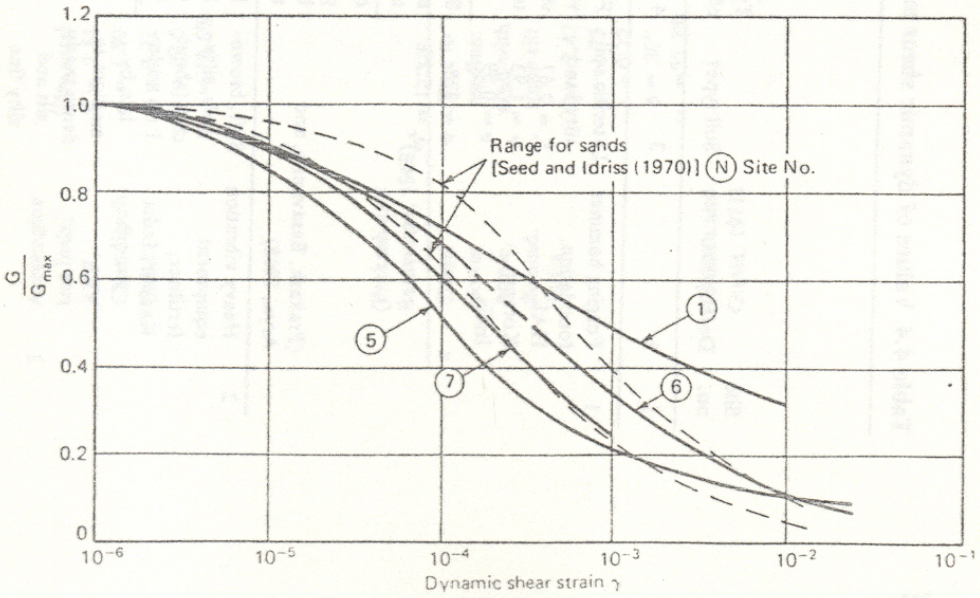

Figure 4.42 Normalized shear modulus (G/G_{max}) vs. shear strain. *(After Prakash and Puri, 1980.)*

Table 4.9 (Continued)

Site no.	Description	Soil type†	Type of test	Size of block or plate	Dynamic shear modulus G, kg/cm^2 from test	Dynamic shear modulus G, kg/cm^2 for confining pressure of 1 kg/cm^2	Associated strain level	Remarks (location)
1	2	3	4	5	6	7	8	9
		ω_c = 17.6% Depth of water table, 4.2 m; followed by a layer of silty clay up to 17.75 m	Forced-horizontal-vibration test	Block: 1.5 × 0.75 × 0.70 m	274.3	757.0	2.0×10^{-4}	θ = 35°
					242.4	668.8	3.0×10^{-4}	θ = 70°
					225.0	621.0	4.6×10^{-4}	θ = 105°
					210.0	578.2	7.3×10^{-4}	θ = 140°
				Block: 1 × 1 × 1 m	221.7	573.6	2.1×10^{-4}	θ = 35°
					193.2	504.0	3.4×10^{-4}	θ = 70°
					180.8	471.7	5.0×10^{-4}	θ = 105°
					168.1	438.5	6.0×10^{-4}	θ = 140°
			Free-vertical-vibration tests	Block: 1.5 × 0.75 × 0.70 m high	647.5	1786.0	1.0×10^{-6}	
				Block: 1 × 1 × 1 m	687.6	1798.0	1.0×10^{-6}	
			Free-horizontal-vibration tests	Block: 1.5 × 0.75 × 0.7 m high	725.3	2001.0	1×10^{-6}	
				Block: 1 × 1 × 1 m high	379.4	990.0	1.0×10^{-6}	
Puri (1969)								

* Prakash and Puri (1980).

† S_s = specific gravity of particles; γ = bulk density of soil; e = void ratio; ϕ = angle of internal friction; ω_c = water content.

‡ θ = angle of setting of eccentric masses.

modulus (defined as G-value at a particular strain, divided by G-value at strain of 10^{-6}) and strain is shown in Fig. 4.42. A similar plot for sands and clays was also made by Richart (1977), who presented a good summary of correlations between dynamic constants and shear strain.

4.15 FINAL COMMENTS

Stress deformation and strength characteristics of soils under static and dynamic loads depend on soil characteristics, such as void ratio, relative density, stress history, and preconsolidation pressure, and on initial static stress level, pulsating stress level, number of stress pulses, and, to a lesser degree, the frequency of loading and the shape of the wave form.

In silts and clays, with an initial safety factor of 1.5 or 2.0 and between 10 and 100 stress pulses, the total stress (static plus dynamic) versus total strain curve is very close to the stress-strain plot under static loading.

The study of shear parameters in oscillatory simple shear shows that cohesion intercepts decrease appreciably in more plastic clays under oscillatory loads and the angle of internal friction remains constant.

Several laboratory and field methods are available for determining soil modulus. The laboratory methods are oscillatory simple or triaxial shear, and resonant column apparatus. A laboratory apparatus to measure the ultrasonic longitudinal and shear wave velocities was reported by Stephenson (1977). The field methods include cross-bore hole tests, up-hole or down-hole tests, surface-wave techniques, block resonance test, and cyclic-plate-load test.

Simple equations have been developed to use available data to make preliminary estimates of the soil modulus at low strain amplitudes for sands and clays. Also, certain noncohesive deposits from in situ tests were studied to determine variations of soil modulus with strains. Therefore, depending upon the strain value associated in a particular problem, a reasonable estimate of the soil modulus can be made. Ishihara (1971) suggested values of strain levels from several field and laboratory tests and the corresponding state of soil (Fig. 4.43). However, it is recommended that the soil modulus be determined for a wide range of strain levels; a suitable value may then be picked. A correction for confining pressure differences between field and test conditions also needs to be made, as per Eq. (4.23).

Woods (1978) compiled a table of advantages and disadvantages of field techniques discussed in the chapter (Table 4.5).

The effect of a high confining pressure on the dynamic soil modulus has not been investigated to any extent. The problem is of great importance in seismic analysis of high earth and rockfill dams, such as the Tehri and Kishau Dams, which are proposed to be built in the Himalayas and will each be about 300 m high. Preliminary work in this direction has been initiated at Roorkee.

In actual analysis of substructures, it is convenient to express the stress-strain curve in a mathematical form. For monotonic loading, Kondner's (1963) hyper-

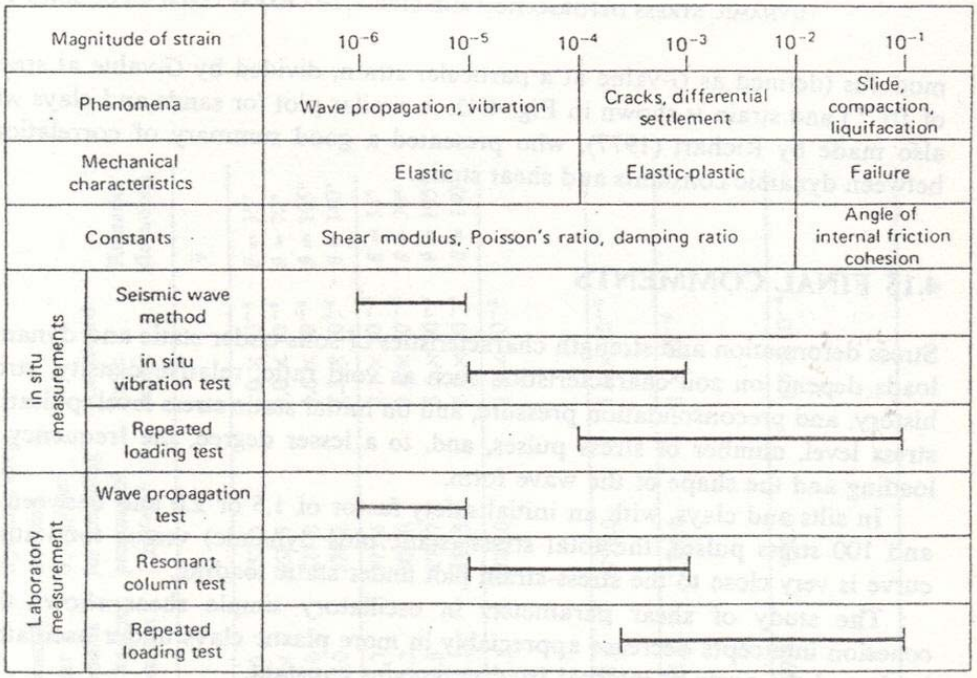

Figure 4.43 Strain level associated with different in situ and laboratory tests. (*After Ishihara, 1971.*)

Table 4.5 Field techniques for measuring dynamic soil properties*

Field technique	*P*-wave velocity	*S*-wave velocity	Other measurements	Advantages	Disadvantages
Refraction	X	X	Depths and slopes of layers	Reversible polarity Works from surface Samples large zone Preliminary studies	Misses low velocity zones Low strain amplitudes Properties measured are for thin zones near boundaries
Cross-hole	X	X		Known wave path Reversible polarity Works in limited space	Need two or more holes Need to survey holes for verticality
Down-hole or up-hole	X	X		One hole only Reversible polarity Finds low velocity Works in limited space	Measures average velocities Ambient noise near surface Low strain amplitude
Surface		X	Attenuation of *R* wave	Work from surface	Uncertain about effective depth Needs large vibrator
SPT			Empirical correlation with liquefaction	Widely available Widely used in past	Needs "standardization"
Resonant footing			Modulus of near-surface soils	Works from surface	Limited depth of influence

*After Woods (1978).

bola has been adopted in several cases. However, for cyclic stress-strain, Richart (1977) and Desai and Christian (1977) recommend the use of the Ramsberg-Osgood (1943) model. The detailed treatment of the subject is beyond the scope of this text.

PRACTICE PROBLEMS

4.1 List and discuss the factors affecting shear strengths of cohesive soils under static and dynamic loads.

4.2 Differentiate between the structure of undisturbed and remolded soils. Draw stress-strain curves for both. If an undisturbed clay sample is vibrated, what type of structure do you expect after the vibrations have ceased?

4.3 What do you understand by a "stress control" and "strain control" type of shear testing device?
(*a*) Is the pendulum loading apparatus a stress control type or a strain control type?
(*b*) Is Seed's apparatus for repetitive load applications "stress" or "strain" controlled?

4.4 Describe the effects of the following on the strength of clayey soils:
(*a*) Number of pulses of loading
(*b*) Wave form of pulsating load
(*c*) One-dimensional and two-dimensional loading
(*d*) Drainage conditions
(*e*) Loading time

4.5 A clay sample, 3.8 cm in diameter and 8 cm long, is subjected to one-dimensional pulsating stress. The frequency of load application is 2 Hz and sustained load is zero.

Draw a typical dynamic stress versus total strain for this sample. Superimpose on this diagram the static stress versus strain in an unconfined test on this sample.

How does this plot differ from the one in Fig. 4.21?

4.6 List and discuss the methods for determining dynamic soil modulus of soils.

4.7 List and discuss the factors on which the soil moduli depend. In a given case, how are corrections for the variations in these factors applied to determine the value for your problem?

4.8 List and discuss the provisions of the Indian Standards for determining dynamic soil modulus. If you were to write a standard of your own, how would you revise these provisions?

4.9 The following tests were performed at the ground surface to determine the value E, the Young's modulus, and C_u, the coefficient of elastic uniform compression for the design of a compressor foundation at a site.

Table 4.6 Vertical-vibration test data

Serial no.	Angle of settling of eccentric masses	f_{nz}, Hz	Amplitude at resonance mm
1	15	35.0	0.06375
2	30	32.0	0.150
3	45	31.0	0.210
4	60	29.5	0.30
5	120	28.0	0.525
6	140	27.0	0.620